

80-1-230
圖書室

DEUTSCHES ELEKTRONEN-SYNCHROTRON **DESY**

DESY 79/79
December 1979

NEW RESULTS IN e^+e^- ANNIHILATION FROM PETRA

by

H. Schopper

NOTKESTRASSE 85 2 HAMBURG 52

To be sure that your preprints are promptly included in the
HIGH ENERGY PHYSICS INDEX,
send them to the following address (if possible by air mail) :

**DESY
Bibliothek
Notkestrasse 85
2 Hamburg 52
Germany**

DESY 79/79
December 1979

NEW RESULTS IN e^+e^- ANNIHILATION FROM PETRA

H. Schopper

Deutsches Elektronen-Synchrotron DESY

Hamburg, Germany

Invited talk at the X International Symposium of Multiparticle
Dynamics, Fort Aguada Beach Resort, Goa (INDIA), September 1979

C o n t e n t s

	page
1) Introduction	1
2) Validity of QED and lepton universality	2
3) Total hadronic cross section, multiplicities and inclusive spectra	3
4) $q\bar{q}$ -jets and search for the t-quark	6
5) Evidence for gluons	12
A) 3 gluon decay of the Y	13
B) gluon bremsstrahlung	16
6) Two-photon process	26
7) Search for free quarks	27

List of references

1) Introduction

The large e^+e^- storage ring PETRA has been operated during 1979 in the energy range from 2×6.0 GeV to about 2×16 GeV. By adding more rf cavities it is hoped that in 1980 the energy can be increased to about 2×19 GeV. The DESY synchrotron is used as injector for electrons and positrons and originally DORIS has been operated as positron accumulator. Since the interest in using DORIS for elementary particle physics and for synchrotron radiation physics is very high, a new little ring PIA (Positron Intensity Accumulator) has been brought into operation in June '79 and hence DORIS will resume its own research programme in fall '79.

The four experiments PLUTO, TASSO, MARK J and JADE are installed in four interaction regions (Fig. 1). By the end of '79 PLUTO may be replaced by CELLO. About 270 physicists are engaged in these experiments, about half coming from other countries, which include mostly European countries, but also groups from USA, Japan, Israel and China.

Naturally all experiments were engaged in the most interesting topics and one may state with satisfaction

that their results agree. However, because of different experimental conditions and ensuing differences in the evaluation of the data it is not always possible to present corresponding data in the same graph. In such cases the data of only one experiment will be presented here, and it should be born in mind that more data exist than those shown here.

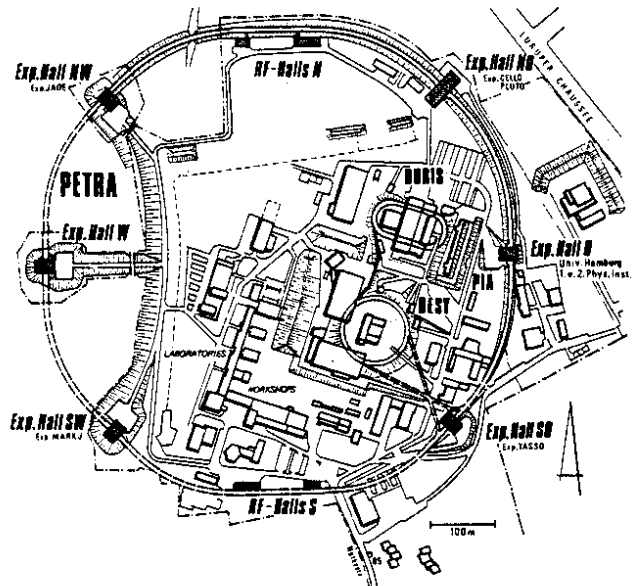


Fig. 1: The DESY site

2) Validity of QED and lepton universality

The angular dependence of elastic e^+e^- (Bhabha) scattering has been measured by all experiments as a function of energy. As an example the results²⁾ of JADE are shown in Fig. 2. If one plots $s \cdot d\sigma/d|\cos\theta|$ the data for different c.m. energies \sqrt{s} should fall on top of each other which is indeed observed. The results agree very nicely with the QED expectation. JADE has also observed the process $e^+e^- \rightarrow \gamma\gamma$ which also is in agreement with QED.

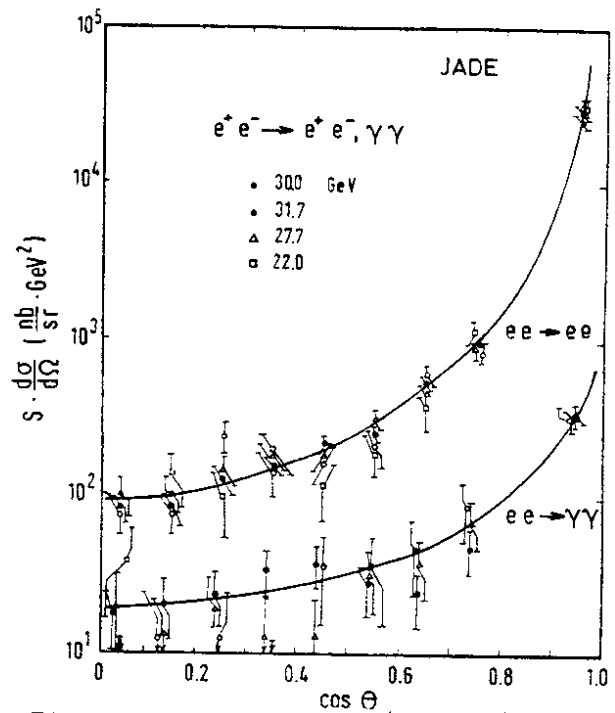


Fig. 2: $s \cdot d\sigma/d\Omega$ for $e^+e^- \rightarrow e^+e^-$ and $e^+e^- \rightarrow \gamma\gamma$ as function of the angle with respect to the incoming beam for four different energies \sqrt{s} .

MARK J has also measured¹⁾ the cross section for $e^+e^- \rightarrow \mu^+\mu^-$ and $e^+e^- \rightarrow \tau^+\tau^-$ (Fig. 3). The angular distribution of these processes agree with the QED predictions for $e^+e^- \rightarrow \mu^+\mu^-$ providing evidence for lepton universality.

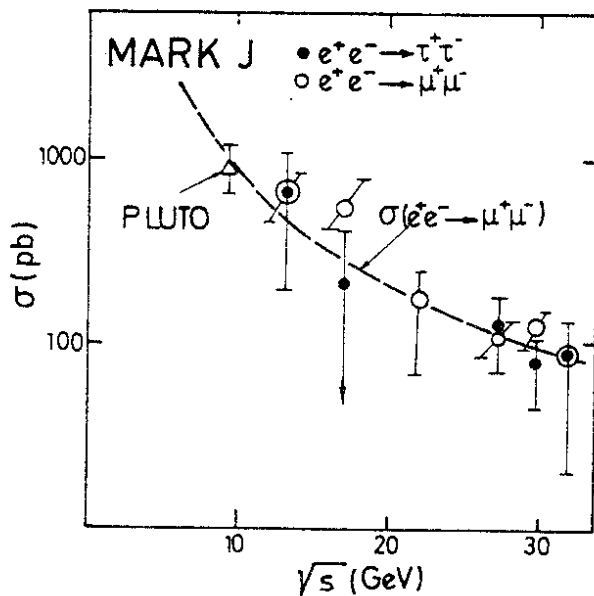


Fig. 3: The cross section for $e^+e^- \rightarrow \mu^+\mu^-$ and $e^+e^- \rightarrow \tau^+\tau^-$ as function of the c.m. energy \sqrt{s} as measured by MARK J.

To express the validity of QED in a quantitative form one has to introduce form factors, e.g.

$$F = 1 \mp \frac{q^2}{q^2 - \Lambda_{\mp}^2}$$

where q is the momentum transfer and Λ_{\mp} is a cut-off parameter. The following table shows the Λ -values obtained by the MARK J experiment¹⁾. These values imply that the leptons e , μ and τ behave like point-like particles to distances of about 10^{-16} cm, a thousand times less than the radius of the proton. It has also been shown⁴⁾ that from the cut-off parameters for $e^+e^- \rightarrow \mu^+\mu^-$ interesting restrictions for the masses of the neutral gauge particles of weak interactions can be derived.

Table 1: Lower limits (95 % C.L.) for the cut-off parameter

	electron	muon	tau
Λ^-	95	97	53
Λ^+	74	71	47

cut-off (GeV)

3) Total hadronic cross section, multiplicities and inclusive spectra

Results for the total hadronic cross section have been obtained by the four experiments^{2,3,5,6,7,26,30)} up to c.m. energies of 31.6 GeV. The PLUTO detector previously working at DORIS has covered the range from 3 to 31.6 GeV, the largest span of energies investigated by a single detector.

The ratio $R = (\sigma(e^+e^- \rightarrow \text{hadrons}) / \sigma(e^+e^- \rightarrow \mu^+\mu^-))$ is shown in Fig. 4. The full lines correspond to the theoretical expectations for different quark charges

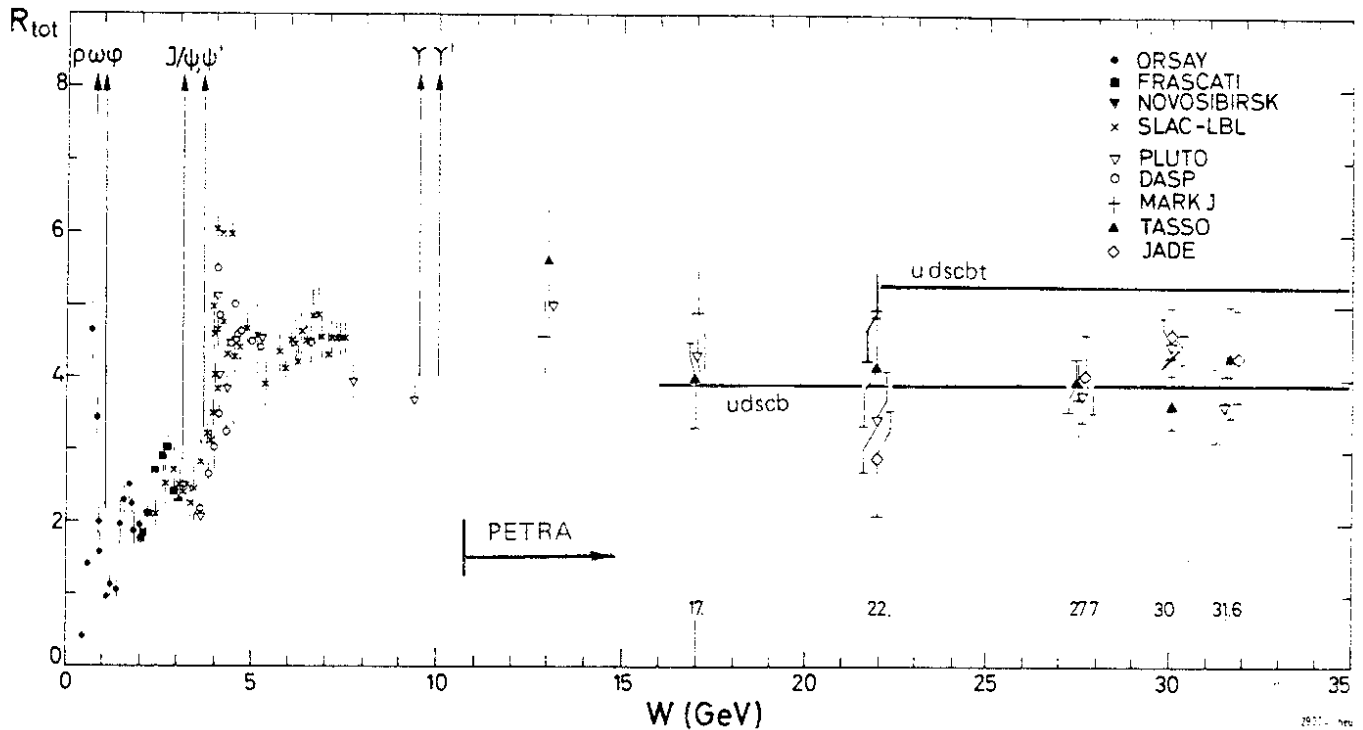


Fig. 4: The ratio $R = \sigma_{\text{tot}}(e^+e^- \rightarrow \text{hadrons}) / \sigma(e^+e^- \rightarrow \mu^+\mu^-)$ as function of the c.m. energy $W = \sqrt{s}$.

Q_i including QCD corrections according to $R = 3 \sum_i Q_i^2 (1 + \alpha_s/\pi)$. The data in the PETRA energy range are consistent with the prediction including a b-quark. There is no evidence for the opening-up of a new threshold corresponding to the t-quark with charge 2/3. Unfortunately the accuracy of the absolute normalization (10-15 %) is not good enough to test the QCD corrections which would require an accuracy of better than 3 %.

In Fig. 5 the average charged multiplicity is presented as a function of the c.m. energy. Whereas it seemed that in the energy range investigated previously the multiplicity increased logarithmically, the PETRA results show that above 10 GeV the

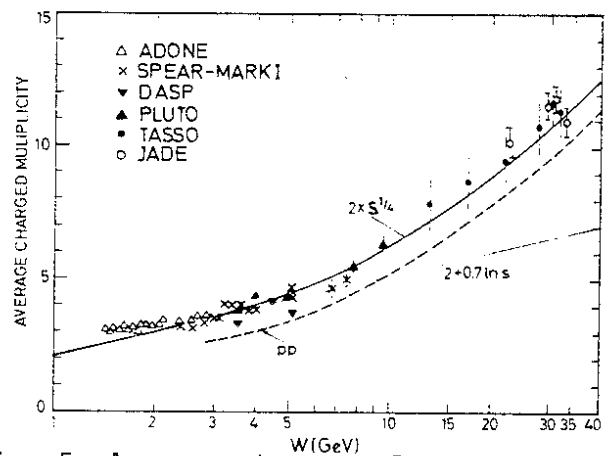


Fig. 5: Average charge multiplicity as function of the c.m. energy $W = \sqrt{s}$. The dotted curve represents the average multiplicity in pp interactions.

rise is faster indicating the presence of a term $(\ln s)^2$. A good fit can also be obtained by the functions $s^{-1/4}$ which is preferred by some theories⁸⁾. It is remarkable that the charge multiplicity in e^+e^- annihilation has a very similar behaviour than that of pp interactions, except that there is a difference in magnitude of about 1 unit.

With respect to inclusive particle production an identification of different kinds of particles has not been achieved yet. Hence only spectra for all charged particles have been measured so far. In Fig. 6a the invariant cross section as a function of rapidity is presented³⁾. As one notices the rapidity

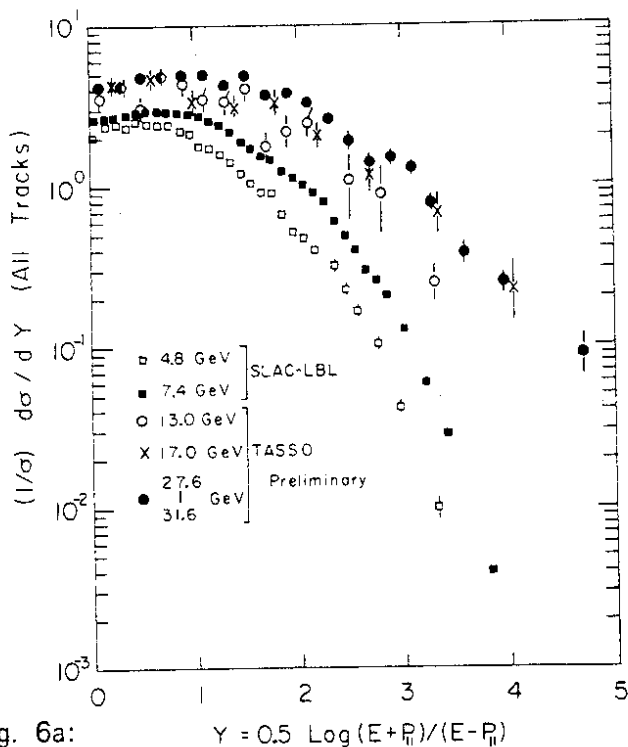


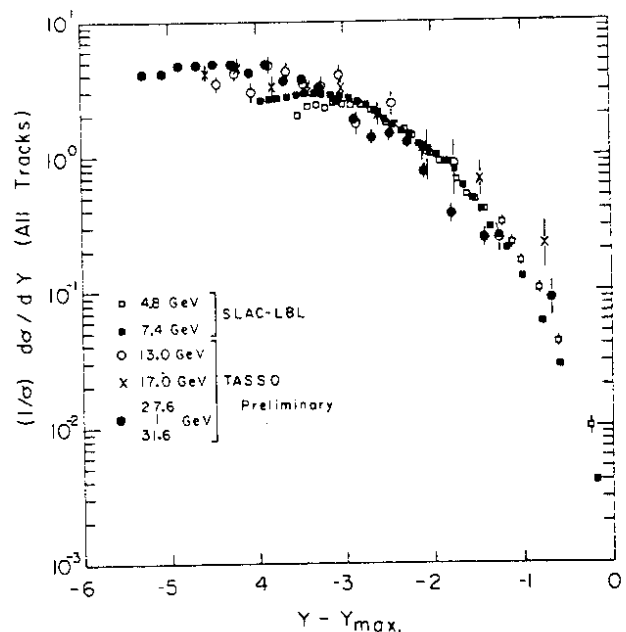
Fig. 6a:

Rapidity distributions for charged particles assuming $m = m_\pi$, measured at 13, 17 and 24.7-31.6 GeV by TASSO³⁾. For comparison data at 4.8 and 7.4 GeV by SLAC-LBL.

Fig. 6b:

Rapidity distributions³⁾ (same as in Fig. 6a) plotted as a function of $Y - Y_{\max}$.

plateau gets longer with increasing energy which is expected. But one sees that the height of the plateau near $y=0$ also rises with energy. This is related to the fact that the average multiplicity increases faster than $\ln s$ (see Fig. 5). In Fig. 6b the invariant cross section has been plotted as function of $Y - Y_{\max}$.



One observes that for Y values close to Y_{\max} the data scale within the experimental errors.

Finally, in Fig. 7 the invariant cross section³⁾ is plotted as function of the normalized momentum $x = p/p_{\text{beam}}$. The data scale for $x > 0.2$. This is expected on the basis of the simple parton model. QCD effects would lead to a breaking of this scaling. However, QCD effects are too small to be detectable with the presently achieved accuracy. For $x < 0.2$ the cross section increases with energy, the data at 13 GeV being larger than at the other energies. Part of this increase is due to the opening up of the b-threshold and it is associated to the rise of the rapidity plateau (cp. Fig. 6a).

4) $q\bar{q}$ - jets and search for the t-quark

At high energies the predominant production process for hadrons is the creation of a $q\bar{q}$ pair and because of confinement these two particles disintegrate into normal hadrons. If the total e^+e^- energy just corresponds to twice a particular quark mass these $q\bar{q}$ pairs are produced practically at rest and hence they decay more or less isotropically. If on the other hand the c.m. energy is much higher than a particular quark threshold the quarks are produced with high velocities and due to the Lorentz-transformation the fragmentation products will appear as jets in the c.m. system. The jets will become the more pronounced the higher the energy if the transverse momentum of the particles with respect to the jet axis is independent of energy. This seems to be borne out⁹⁾ by hadron-hadron interactions and deep inelastic

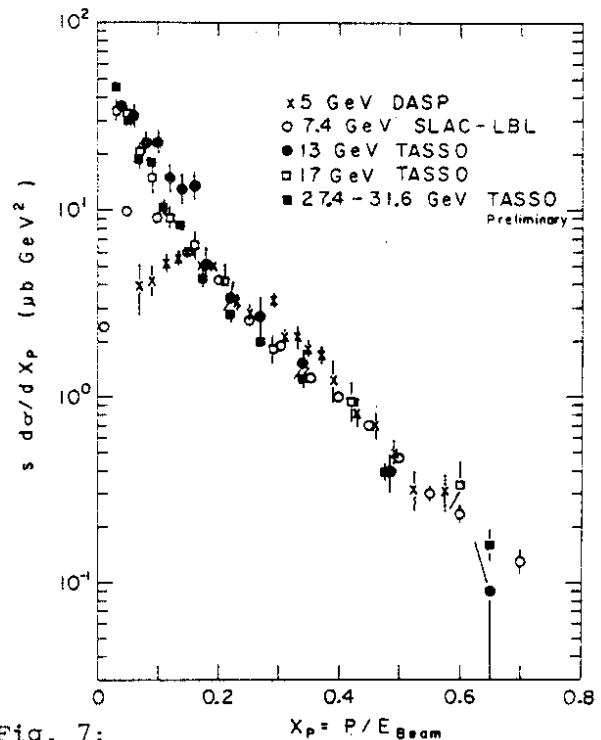


Fig. 7:
The cross section $s \cdot d\sigma/dx$ ($x = P/E_{\text{beam}}$) for inclusive charged particle production measured in the TASSO experiment at 13, 17 and 27.4-31.6 GeV and at 5 GeV (DASP) and 7.4 GeV (SLAC-LBL).

scattering where it was found that a reasonable parametrization of the probability of a quark to disintegrate into a particle with momentum p is given by⁹⁾

$$f(z, p_{\perp}) = D(z) \cdot e^{-(p_{\perp} |2\sigma_{\perp})^2}$$

where $z = p/q$ is the fraction of the original quark momentum q and the transverse momentum distribution is characterized by σ_{\perp} .

If the quark spin is $1/2$ one expects an angular distribution of the jet axis with respect to the incoming beam of the form

$$d\sigma/d|\cos\theta| \approx 1 + \cos^2\theta + P^2 \sin^2\theta \cos 2\phi$$

where P is the transverse polarization of the beams. If the quark spin were zero the angular distribution would be proportional to $\sin^2\theta$.

In order to characterize the jet-like topology of events a number of variables are used. Most commonly used are the sphericity S and thrust T which are defined as

$$S = \frac{3}{2} \frac{\min \sum p_{i\perp}^2}{\sum p_i^2}$$

$$T = \frac{\max \sum |p_{i\parallel}|}{\sum |p_i|}$$

where the summation goes over the particles.

The definition implies that an axis of the jet is determined which minimizes $\sum p_{i\perp}^2$ or maximizes $\sum |p_{i\parallel}|$, respectively. $p_{i\perp}$ and $p_{i\parallel}$ are the transverse and longitudinal momenta with respect to this axis. Theorists prefer T since it is a quantity linear in the momenta and hence free of divergencies in field theories. The analysis of the experimental results has shown that in most cases it does not matter much which of these quantities is used. For small values of S one has approximately $1 - T \approx S$ and S is related to the opening angle δ of a jet by $S \approx (3/2)\langle\delta^2\rangle$. For collinear

events $S \rightarrow 0$ and $T \rightarrow 1$, whereas for spherical events $S \rightarrow 1$, $T \rightarrow 1/2$. If the fragmentation of quarks is characterized by a constant p_{\perp} one would expect that with increasing energy $S \sim 1/W^2$ where W is the c.m. energy.

The experimental results can be summarized in the following way. The angular distribution³⁾ of the jet axis with respect to the incident beam is in agreement with the expected $1+\cos^2\theta$ distribution expected for spin 1/2-quarks (Fig. 8). Recently a transverse polarization of the beams in PETRA has been observed at high energies which is due to the emission of synchrotron radiation. In Fig. 9 the azimuthal distribution of the thrust axis is shown, as observed by JADE²⁾. It agrees nicely with the formula given above and corresponds to beam polarizations of $(85 \pm 15) \%$.

The average sphericity $\langle S \rangle \approx 1 - \langle T \rangle$ as function of the c.m. energy is presented^{3,6,11,26,27)} in Fig. 10. Quantitatively one finds that indeed $\langle S \rangle$ decreases with increasing $W = \sqrt{s}$ implying that the 2-jet character of the events becomes more pronounced. However, at large energies $\langle S \rangle$ does not decrease like $1/W^2$ as expected in the naive jet model described above but the dependence is approximately like $1/\sqrt{W}$. This is in agreement with the QCD expectation²⁸⁾.

Around 4 and 10 GeV steps in $\langle S \rangle$ are observed because of the opening of the charm and bottom threshold, respectively. A much larger step is expected for the t-quark threshold since this quark is supposed to have charge 2/3 and because of its high mass the Lorentz boost is small. No such step is seen implying that the $t\bar{t}$ -threshold is higher than about 32 GeV. This does not yet exclude bound $t\bar{t}$ -states 1 or 2 GeV below this limit since they have a very narrow width and could have been missed. In order to clarify this point

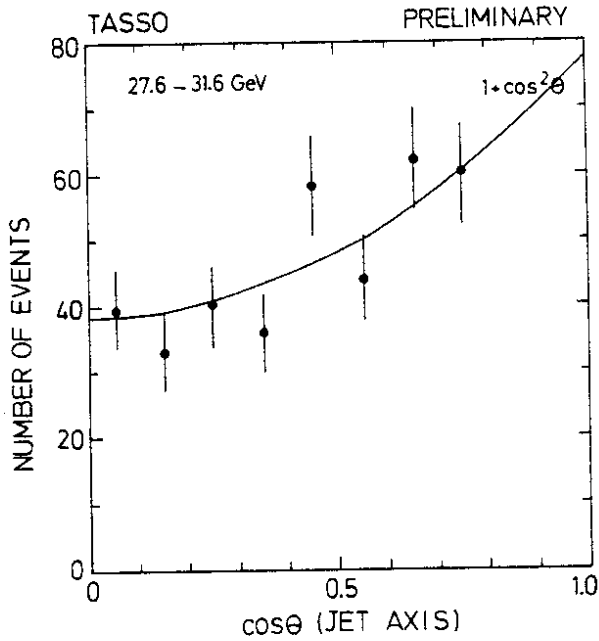


Fig. 8: Angular distribution of the jet axis with respect to the beam as measured by TASSO³). For quark spin 1/2 one expects a $1 + \cos^2 \theta$ distribution.

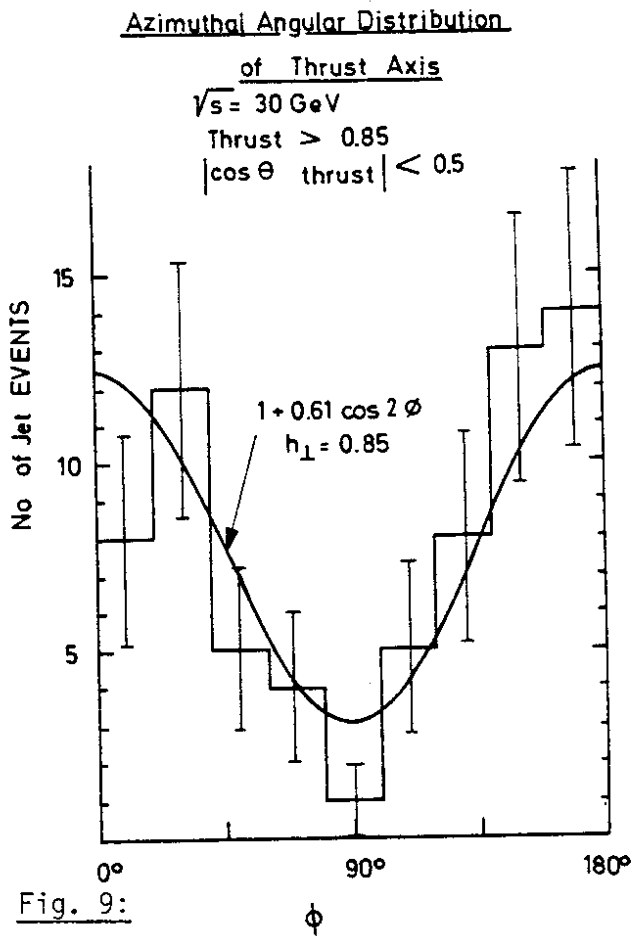


Fig. 9: The azimuthal distribution of the thrust axis at 30 GeV giving evidence for transverse beam polarization of about 80% (JADE coll.).

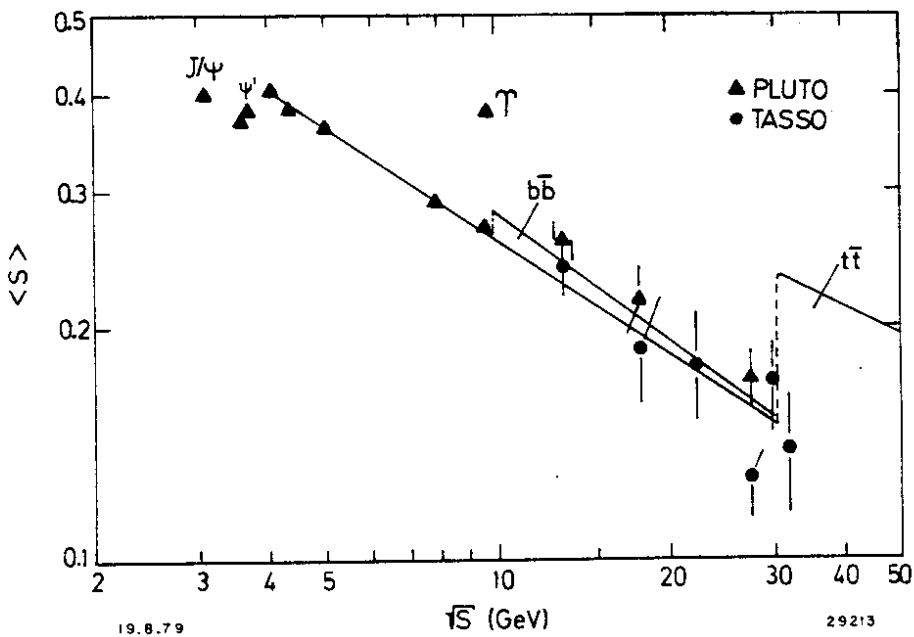


Fig. 10: The average sphericity as a function of the c.m. energy. The curves indicate the expected contributions from u, d, s, c, b and t quarks including QCD corrections. No $t\bar{t}$ -threshold is seen. The sphericity of the Y-resonance is much higher than that of the continuum indicating a different type of event.

a fine scan (in steps of 20 MeV) is planned *) for the region between 30 to 32 GeV. In 1980 it is hoped to bring the PETRA energy up to 38 GeV and a search for the t-quark in that region will be carried out.

In Fig. 11a the distribution of T-values at different energies are shown as an example and similar results were obtained by other experiments^{3,30}). They are compared to the expectations of the Feynman-Field fragmentation model⁹) which has been extended to take into account the fragmentation of the c and b quark in addition to u, d and s. For the highest energy of 31.6 GeV the thrust distribution including the t-quark is also shown. The data are not in agreement with the opening-up of the $t\bar{t}$ -threshold but rather

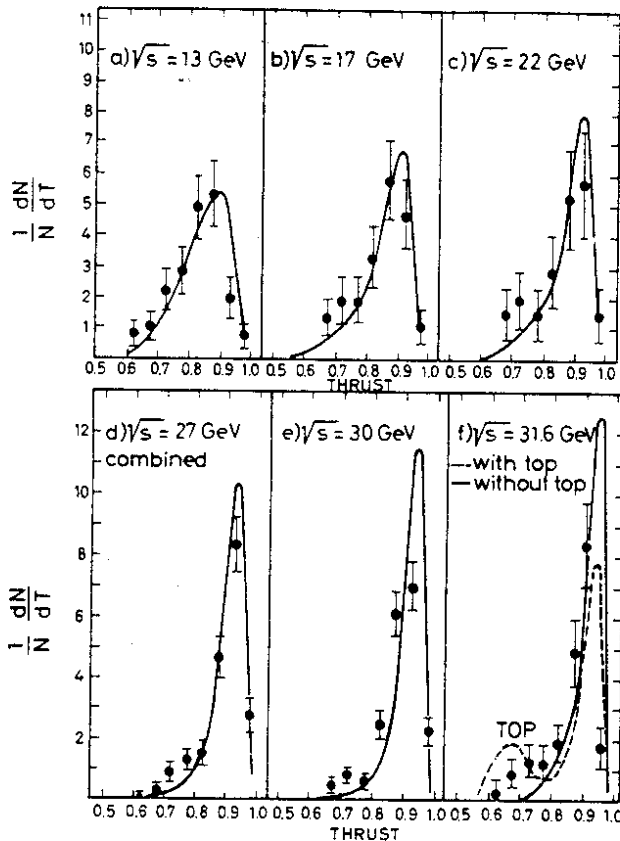


FIG. 11a

Fig. 11a:

The thrust distributions as measured^{5,6,13}) by MARK J at different energies. The solid curves are predictions based on u,d,s, c and b quarks. The dashed curve includes the t-quark contribution.

*) Note added in proof: a scan has been carried out from 29.90 to 31.46 GeV, giving no evidence for a bound $t\bar{t}$ -state. The limit¹²⁾ is $\Gamma_{ee} \cdot B_h < 1.6 \text{ keV}$.

corroborate the absence of the t-quark as established from the average $\langle S \rangle$ distribution.

A closer inspection of Fig. 11a shows, however, a trend of the data to lie somewhat high at the left tail of the T-distribution. To clarify this point the data (with a somewhat more rigorous cut on the visible energy) are compared to theoretical distributions including the emission of gluons (Fig. 11b).

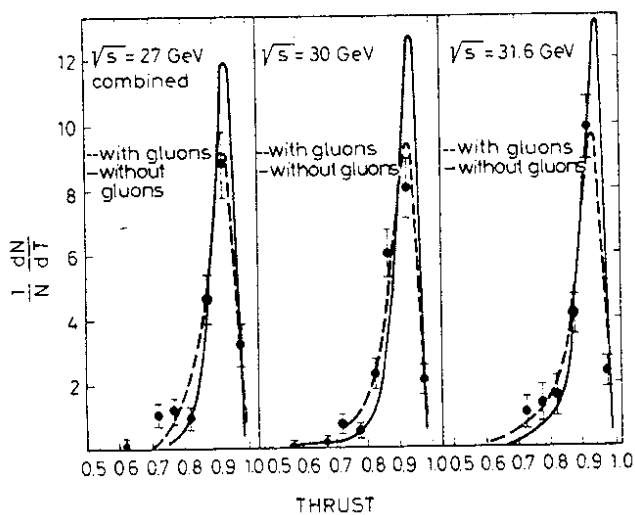


Fig. 11b:

The thrust distributions as measured^{5,6,13}) by MARK J at different energies.

Data at higher energies (and somewhat different cuts than in a)). Full curves: predictions for u,d,s,c,b quarks without gluon emission, dotted curve: with gluon emission.

The excess of events at low thrust can very well be explained by gluon emission and cannot be regarded e.g. as an indication for the existence of another quark with charge $1/3$.

There is no real theory to predict the mass of the t-quark. Many guesses have been made, however, and most predictions center around an energy of about 28 GeV for the lowest bound $t\bar{t}$ -state. Indeed, it is tantalizing that the ratios between the lowest bound states $(c\bar{c}) / (s\bar{s}) = 3.037$ and $(b\bar{b}) / (c\bar{c}) = 3.054$ are so close together and assuming $(t\bar{t}) / (b\bar{b}) = 3.04$ one arrives at $(t\bar{t}) = 28.8 \text{ GeV}/c^2$. Similar values have been obtained from estimates involving weak mixing angles¹⁴). As mentioned above, such a bound state near 28 GeV cannot be excluded before

a scan has been made^{*)}, but its existence seems unlikely. From considerations involving higher symmetries¹⁴⁾ the relation

$$\frac{m(t)}{m(b)} = \sqrt{\frac{m(u) \cdot m(c)}{m(d) \cdot m(s)}}$$

has been derived which would result in a mass ($t\bar{t}$) $\approx 54 \text{ GeV}/c^2$ lying beyond the PETRA energy range.

5) Evidence for gluons

A crucial test for quantum chromodynamics (QCD) is the existence of gluons, the field quanta of the strong interaction. Since gluons like quarks carry colour charge it would not be possible to observe free gluons if only colour neutral objects exist in nature ('confinement'). One expects that gluons would fragment into ordinary hadrons analogously to quarks. However, a gluon can be considered to fragment in a first step into a $q\bar{q}$ pair which then would disintegrate into hadrons. Consequently the gluon jets are expected to have a higher multiplicity and lower average momentum for a given energy.

There are two possibilities to observe gluon jets both of which have been exploited recently:

- A) The decay of a bound vector state into 3 gluons $V \rightarrow 3 g$. In analogy to orthopositronium a spin 1 state decays into at least 3 field quanta, but not 2. The gluon jets will be the more pronounced the higher the mass m_V is since the more energy will be available for each jet. A heavy $t\bar{t}$ state would be an ideal source for 3 gluon jets. As long as it has not been found the Y particle with $m_Y = 9.45 \text{ GeV}/c^2$ offers the only possibility.

^{*)} See footnote on page 10.

B) Because of the analogy between QED and QCD a fast quark should be able to emit gluon bremsstrahlung in a similar way as an electron emits electromagnetic bremsstrahlung. A favourable possibility to look for gluon bremsstrahlung are 2 quark jets at high energies. If the quarks are produced with sufficient energy there is a chance that one of them produces a gluon. In the first instance this would broaden one of the quark jets and finally if emitted at a large enough angle with respect to the quark momentum a 3-jet pattern should evolve.

A) Three gluon decay of the Y

The direct decay of the Y particle into hadrons has been observed at DORIS II (single ring operation); by the experiments PLUTO¹⁵⁾, DASP II¹⁶⁾ and the NaI-lead glass detector¹⁷⁾. The latter two experiments have also obtained data for the Y'. The experimental details cannot be discussed here and neither the subtraction procedure for the 2 jet-continuum underneath the resonance (see¹¹⁾).

Since only 9.45 GeV are available in total the average jet energy is only about 3 GeV. With such a low energy one cannot expect 3 pronounced, well separated jets, but rather they will overlap considerably. As a consequence an elaborate statistical analysis is required to find the 3-jet structure.

Various kinematical variables have been introduced for that purpose. One of them is triplicity T_3 which is a generalization¹⁰⁾ of thrust to 3 jets

$$T_3 = \max \left\{ \left| \sum_{c_1} p_i \right| + \left| \sum_{c_2} p_i \right| + \left| \sum_{c_3} p_i \right| \right\} / \sum_{\text{all}} |p_i|.$$

It ranges from $T_3 = 1$ (perfect 3 jets) to $T_3 = 3 \sqrt{3}/8 = 0.65$ (spherical event).

The particles are grouped into 3 non-empty classes C_i . The classes C_i yielding the maximum T_3 are identified with the 3 hadron jets. Once the three jets have been determined in this way the angle between 2 jets or the energy of each jet can be used as variables.

The PLUTO results¹¹⁾ for the direct Υ -decays are shown in Fig. 12. In the same figure results are included which were taken just off the Υ -resonance.

The experimental data which have rather small statistical errors are compared

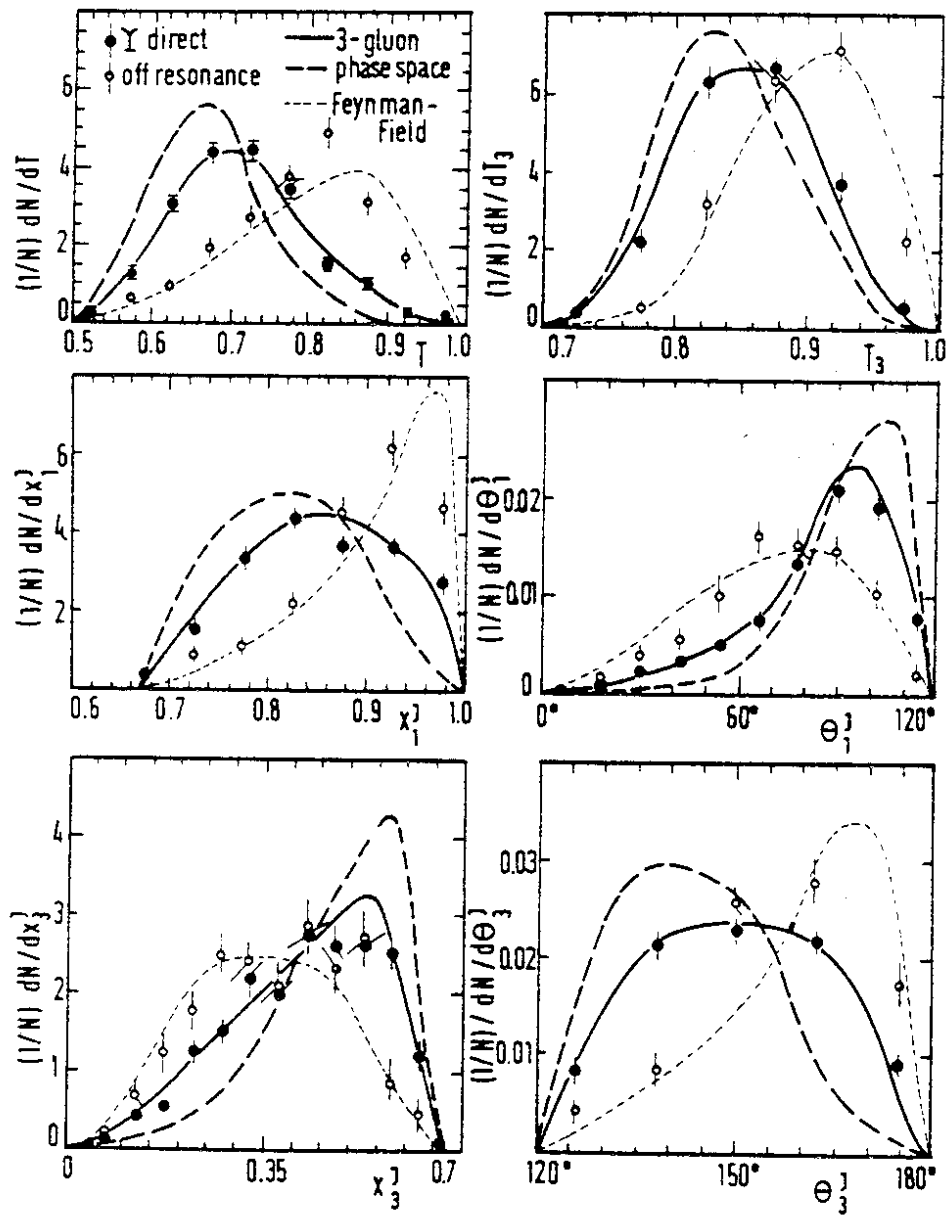


Fig. 12: Experimental distributions of thrust T , triplicity T_3 , reconstructed gluon energies x_1^J , x_3^J and reconstructed angles θ_1^J , θ_3^J between gluons compared to predictions based on various models for the Υ direct decays and for continuum events (PLUTO experiment).

to three models. The 3 gluon decay according to the QCD expectation, the 2 jet model and a simple statistical model. As one notices for all variables the direct Y -decay data agree very nicely with the assumption of 3 gluon decays. On the other hand, they disagree completely with the 2 jet model, which, however, describes very well the off-resonance data. The statistical model is in disagreement with both sets of data and is ruled out. Of course a more sophisticated statistical model including clusters or resonances may be invented to describe the Y -decay. This has not been done so far and it would probably contain a number of arbitrary assumptions and several free parameters. The analysis given in Fig. 12 can be refined by Dalitz-plot-like investigations¹¹⁾, but this would be beyond the scope of this review.

Very important information on the gluon spin can be obtained from the angular distribution of the axis of the most energetic jet with respect to the beam axis. For a vector gluon (spin 1) as required by QCD one expects¹⁸⁾ a distribution of the form $1 + 0.39 \cos^2\theta$, whereas for a scalar gluon (spin 0) it would go like $\sin^2\theta$. The experimental data¹¹⁾ (Fig. 13) agree nicely with the expectation for the vector gluon and exclude a scalar gluon. This finding has been corroborated by a Dalitz-plot analysis¹¹⁾.

In conclusion it can be stated that the hadronic decay of the Y -particle has not only given evidence for 3 gluon jets, but indications for the vector character of the gluon have also been obtained.

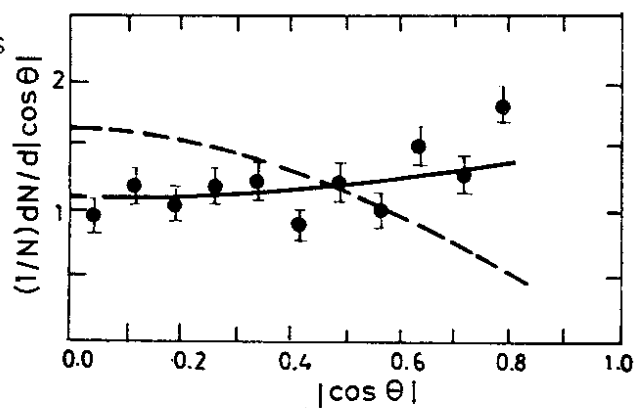


Fig.13

The angular distribution of sphericity axis relative to the incident beam for Y direct decays. Predictions for gluon spin 1 (full curve) and spin 0 (broken curve).

B) Gluon bremsstrahlung

The emission of gluons in the production and fragmentation of a $q\bar{q}$ pair manifests itself in a number of ways. Starting with global features and proceeding to detailed patterns one arrives at the following list:

- 1) The average transverse momentum $\langle p_{\perp} \rangle$ of a jet is expected to increase approximately linearly with the c.m. energy W . It is remarkable that here a linear QCD effect occurs, whereas most QCD effects have a log-dependence.
- 2) The increase of $\langle p_{\perp} \rangle$ should be due to comparatively few events, since hard gluon emission is a rare process ($\sim 10\%$). The p_{\perp} -distribution should therefore develop a tail with increasing W .
- 3) Only one jet broadens with increasing W , since the emission of 2 gluons (one by each quark) is a rare process ($\alpha_s < 1$).
- 4) The comparatively large p_{\perp} of the gluon is transferred in the fragmentation process preferentially to hadrons carrying a large fraction of the original quark momentum (sea gull effect).
- 5) The emission of a gluon by a $q\bar{q}$ pair is a process obeying 3 body kinematics and hence the events have to be planar.
- 6) If the gluon is emitted at a sufficiently large angle with respect to the quark momentum the 3-jet pattern should become visible.
- 7) The observed size of the cross section for gluon bremsstrahlung should be consistent with QCD prediction.
- 8) As a consistency check one expects that the transverse momenta relative to the 3-jet axis are 'normal', i.e. those found in ordinary $q\bar{q}$ jets ($\langle p_{\perp} \rangle \approx 300$ MeV, independent of energy).

In the following the experimental data referring to these predictions of QCD will be reviewed. Obviously the most relevant criteria are number 5 and 6.

In Fig. 14 the TASSO results^{3,19)} for $\langle p_T^2 \rangle$ are shown as a function of the c.m. energy W . Similar results were obtained by PLUTO²⁰⁾. $\langle p_T^2 \rangle$ increases considerably with W in agreement with the QCD prediction²⁹⁾ (point 1) and in contrast to $q\bar{q}$ jets without gluon emission, where $\langle p_T^2 \rangle \approx \text{constant}$ is expected.

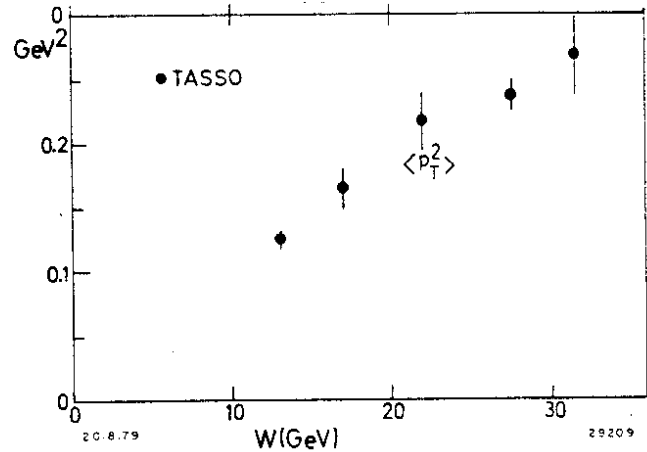


Fig. 14: The dependence of $\langle p_T^2 \rangle$ on the c.m. energy $W = \sqrt{s}$, as measured by TASSO.

In Fig. 15 the distributions of $\langle p_T^2 \rangle$ are shown for two different energy ranges^{3,19)}. Whereas for very low $\langle p_T^2 \rangle$ the experimental points for the two energies agree the tail at high $\langle p_T^2 \rangle$ becomes much more pronounced at 30 GeV. This implies that the increase of the average $\langle p_T^2 \rangle$ is due to relatively few events with high p_T as expected for gluon emission (point 2).

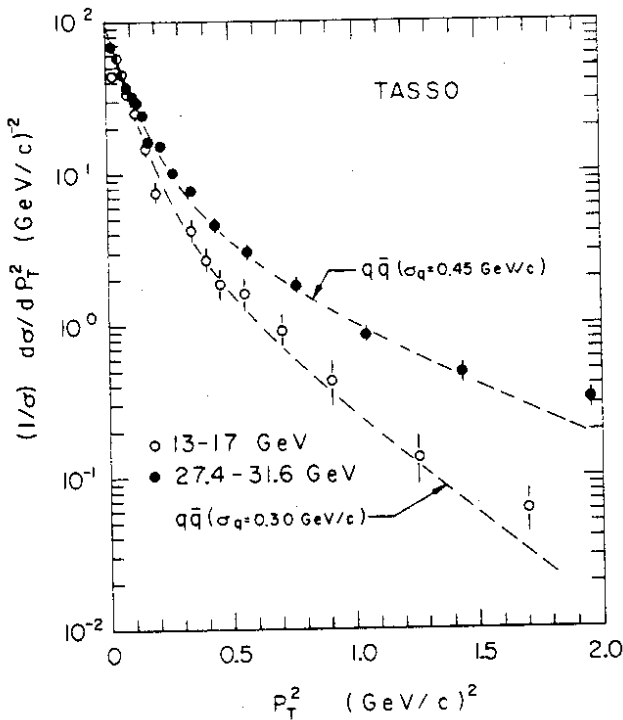


Fig. 15: The distribution of p_T^2 for two different energy ranges. The dashed curves are the expectations for two different parameters σ_q in the quark fragmentation function.

In Fig. 16 the dependence of $\langle p_{\perp}^2 \rangle$ of the energy W is shown for the slim and broad jet separately, as observed by PLUTO²⁰⁾. Similar results were obtained by TASSO^{3,19)}. Because of statistical fluctuations and the selection procedure applied for the two kinds of jets one cannot expect that even without gluon emission the two jets should have the same $\langle p_{\perp}^2 \rangle$. However, it is remarkable that the energy dependence is completely different. Whereas $\langle p_{\perp}^2 \rangle$ of the slim

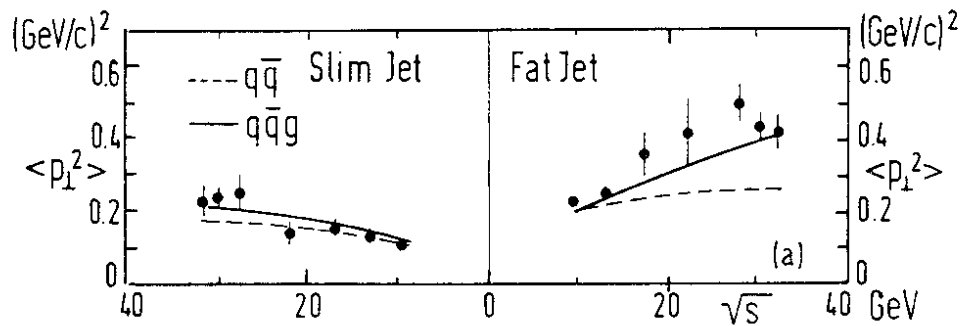


Fig. 16: Average observed $\langle p_{\perp}^2 \rangle$ of charged particles in the slim and fat jet, respectively, as function of the c.m. energy W , as measured by PLUTO.

jet increases only slightly it grows by a factor of two for the broad jet (point 3).

Finally the expectation has been tested if the quark momentum is transferred preferentially to hadrons with large momentum ('sea gull effect'). The PLUTO results²⁰⁾ (with TASSO having produced similar data^{3,19)}) are shown in Fig. 17. Again it is found that p_{\perp} increases essentially in the fat jet and there mainly for large $x_p = p/p_{\max}$ (point 4).

All these observations concerning the change of p_{\perp} with c.m. energy W or normalized particle momentum x are in nice agreement with the QCD expectations. However, as has been indicated in Figs. 14 to 17, an alternative explanation, although unlikely, cannot be excluded entirely. This is the assumption that $\langle p_{\perp} \rangle$ of the jet fragmentation increases with W . If σ_q of the fragmentation function is adjusted properly, an acceptable fit to the data can be obtained.

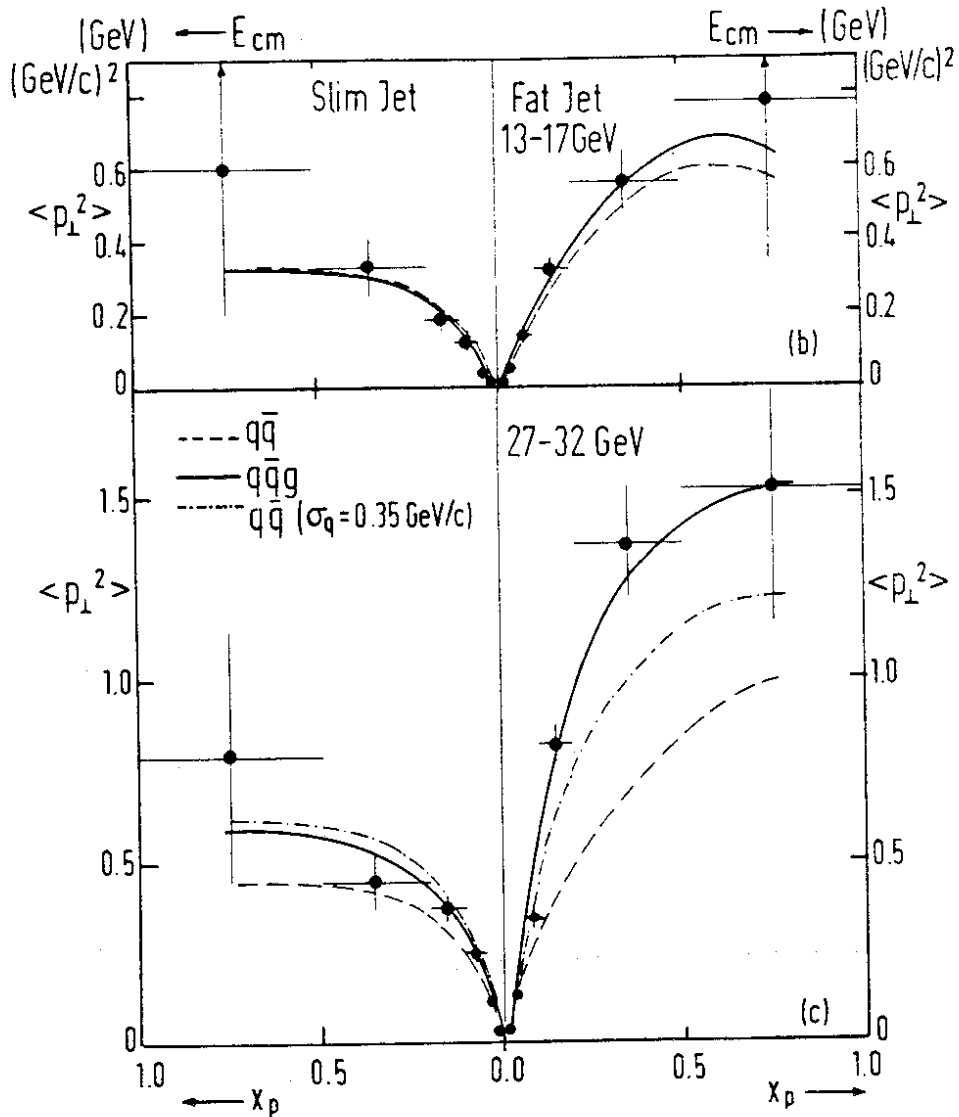


Fig. 17: Plots of $\langle p_{\perp}^2 \rangle$ of charged particles as function of $x_p = p/p_{\max}$ for slim and fat jets in two separate energy ranges as observed by PLUTO. The solid and dashed lines are $q\bar{q}g$ and $q\bar{q}$ predictions, respectively. The dotted-broken line is calculated for $q\bar{q}$ jets with an abnormally high parameter σ_q of the quark fragmentation.

There is no theoretical argument for such a dependence, however. Nevertheless the data presented so far cannot be taken as final proof for the existence of gluons. Hence one has to look for more specific gluon signatures.

Very characteristic for the emission of a gluon by one quark of a $q\bar{q}$ pair is the fact that because of momentum conservation the momenta of the three particles $q\bar{q}g$ have to be coplanar. The resulting 3 hadron jets therefore should yield a planar event. If the gluon is emitted at large enough an angle with

respect to the quark momentum one should be able to observe the three-jet pattern in the event plane.

To describe the flatness of events various variables have been introduced. Only two will be considered here. By determining the thrust axis of an event one can find the most energetic jet. If the remaining momenta are projected on a plane perpendicular to the thrust axis one can determine in this plane the direction of the largest $\langle p_{\perp}^2 \rangle$. This direction together with the thrust axis determines the event plane, and the transverse momentum with respect to the thrust direction lying in the event plane is called $p_{\perp in}$. The momentum perpendicular to the event plane is designated by $p_{\perp out}$ (Fig. 18).

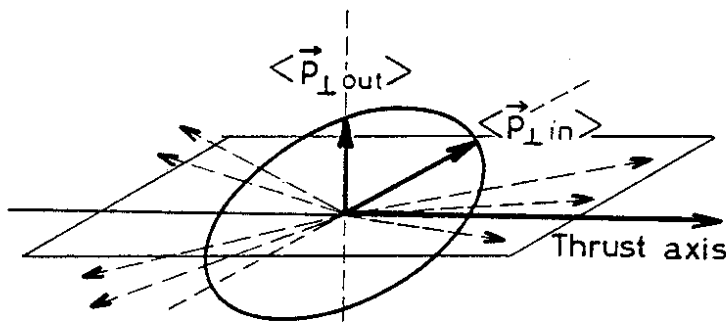


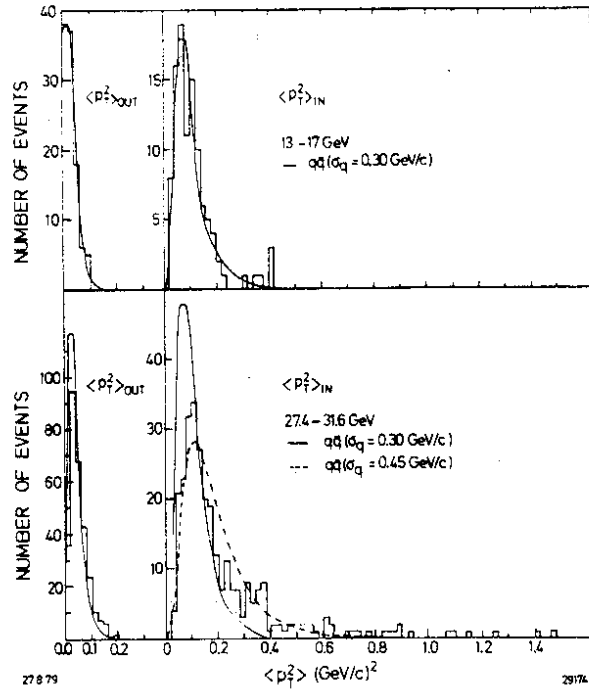
Fig. 18:
Schematic representation of a 3 jet event. The thrust axis and $\langle \vec{p}_{\perp in} \rangle$ determine the event plane. For a planar event one expects $\langle p_{\perp out}^2 \rangle \ll \langle p_{\perp in}^2 \rangle$.

Two-jet events are symmetric around the thrust axis and hence $\langle p_{\perp in}^2 \rangle \approx \langle p_{\perp out}^2 \rangle$. For a flat event one expects $\langle p_{\perp in}^2 \rangle \gg \langle p_{\perp out}^2 \rangle$.

Evidence for planar events was first obtained by TASSO¹⁹⁾. In Fig. 19 the distribution for $p_{T in}^2$ and $p_{T out}^2$ are displayed for the two energy ranges 13-17 and 27.4 to 31.6 GeV. In the lower energy range the measured distributions agree nicely with the $q\bar{q}$ fragmentation model. The $p_{T in}$ distribution is somewhat wider than the $p_{T out}$ distribution which is due to statistical fluctuations in the fragmentation process and to the selection procedure for $p_{T in}$. In the 30 GeV range, however, the $p_{T in}$ distribution develops a long tail whereas the $p_{T out}$ distribution remains normal. The long tail cannot be explained by $q\bar{q}$ fragmentation even if the average $\langle p_{\perp} \rangle$ of the fragmentation process is

Fig. 19:

The mean transverse momentum squared normal to the event plane $\langle p_{\perp}^2 \rangle_{\text{out}}$ and in the event plane $\langle p_{\perp}^2 \rangle_{\text{in}}$ per event for the low and the high energy data as observed by TASSO. The curves show the predictions of the qq model with $\sigma_q = 0.3 \text{ GeV}/c$ (solid) and $0.45 \text{ GeV}/c$ (dashed).



increased (dashed curve). The events in the tail have to be attributed to a planar process, indicating gluon emission at high energies whereas no effect is seen at lower energies. Similar data have been obtained by other experiments^{2,20}.

In the MARK J detector²¹) the energy flow is measured calorimetrically and not the momentum. Also a different variable is used to characterize the events. The oblateness is defined by

$$\sigma = \frac{|\vec{E}_{\text{in}}| - |\vec{E}_{\text{out}}|}{E_{\text{vis}}}$$

where \vec{E}_{in} and \vec{E}_{out} are the directed energy flows (Poynting vector) in the directions defined in Fig. 18 and E_{vis} is the total visible energy of the event. For events containing 3 separated jets one has $\sigma \approx 2 \langle p_{\perp \text{gluon}} \rangle / W$, where $p_{\perp \text{gluon}}$ is the transverse gluon momentum with respect to the quark momentum and W is the c.m. energy. The interesting property of the oblateness lies in the fact that details of the properties of the fragmentation function cancel out. This assertion was corroborated by Monte-Carlo calculations for some important cases.

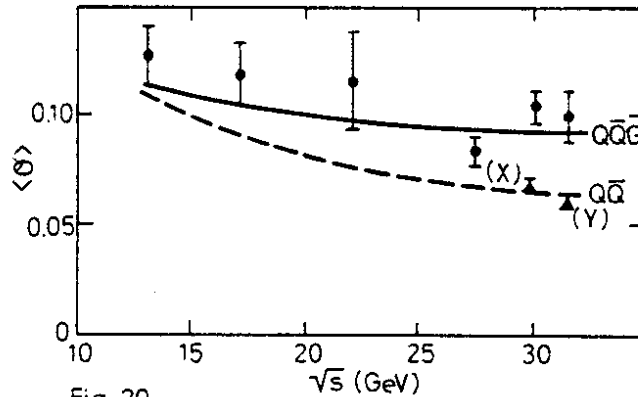


Fig. 20: The average oblateness $\langle \sigma \rangle$ as function of \sqrt{s} compared with the prediction of $q\bar{q}$ (dashed curve) and $q\bar{q}g$ model (full curve). Experimental points from the MARK J experiment. Also shown are points in the $q\bar{q}$ model under different conditions:
 point X: $\langle p_{\perp} \rangle = 425$ MeV instead of 325 MeV, fragmentation function $D(z) = (1-z)^2$;
 point Y: $\langle p_{\perp} \rangle = 325$ MeV, $D(z) = \text{const.}$ for c and b quarks.

In Fig. 20 the dashed line indicates the expectation of $\langle \sigma \rangle$ for the normal $q\bar{q}$ fragmentation model ($\langle p_{\perp} \rangle = 325$ MeV, $D(z) = (1-z)^2$). Point X indicates the σ -value if $\langle p_{\perp} \rangle$ is increased to 425 MeV. If the fragmentation function is changed drastically ($D(z) = \text{const}$ for c and b quarks) point Y is obtained. In both cases only a very small change of $\langle \sigma \rangle$ is indeed produced. The experimental points of the average $\langle \sigma \rangle$ shown in Fig. 20 completely disagree with the $q\bar{q}$ model but agree very nicely with the assumption of gluon emission which yields higher σ -values, i.e. flatter events.

In Fig. 21 the σ -distributions are displayed for the two energy ranges. Here one notices in a very convincing way the agreement of the experimental data of MARK J²¹⁾ with the assumption of gluon emission whereas the different versions of the $q\bar{q}$ model are ruled out. Indeed the oblateness seems to be sensitive enough to indicate gluon emission even at 17 GeV.

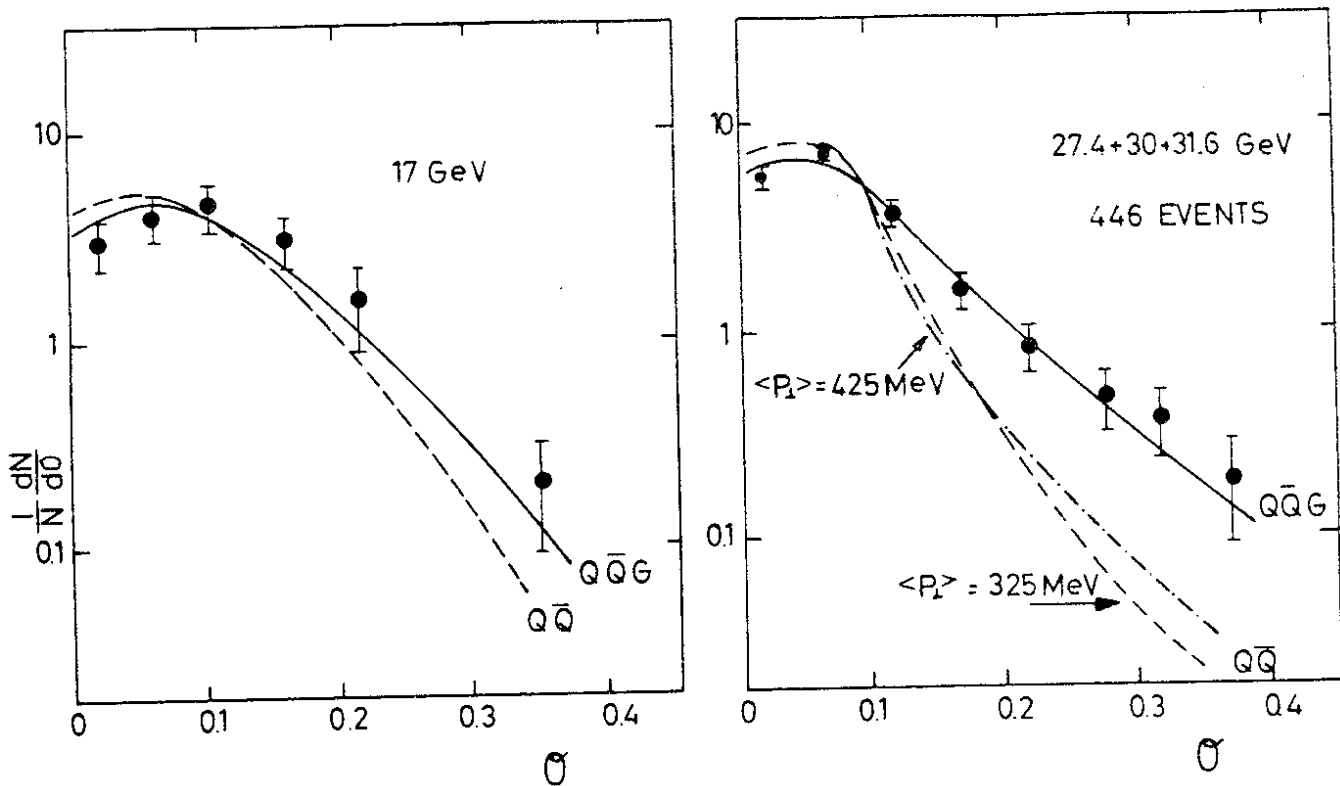


Fig. 21: Oblateness distribution as observed by the MARK J experiment for two different energy ranges. The solid curves are predictions based on the qqg model and the dashed curve on the standard $q\bar{q}$ model ($\langle p_{\perp} \rangle = 325 \text{ MeV}$). The dashed-dotted curve corresponds to the $q\bar{q}$ model with $\langle p_{\perp} \rangle = 425 \text{ MeV}$.

In conclusion the data of all experiments show the existence of planar events (point 5 of the list) and the quantitative results are in good agreement with gluon emission. A more detailed analysis of flat events by means of Dalitz-plots^{3,19,20,22)} cannot be discussed here.

Finally one would like to see the 3-jet pattern (point 6 of the list). All experiments have seen some events which display quite convincingly the three jets and one example is shown in Fig. 22. MARK J has provided²¹⁾ the first statistically relevant observation of the 3-jet pattern. In Fig. 23a) a polar diagram of the energy flow in the event plane is shown. Different events have been oriented by putting the thrust axis on top of each other and making the second largest jets to lie on the same side. Planar events were selected by the cuts $T < 0.8$ and $\theta > 0.1$. The 3-jet structure can be seen. To show in a

Fig. 22:

Example of a 3-jet event (PLUTO). Momentum vectors of an event ($E_{cm} = 31.6$ GeV) with high triplicity and low thrust projected onto the triplicity plane (top left), onto a perpendicular plane normal to the fastest jet (top right) and onto a plane containing the direction of the fastest jet (bottom). Solid and dotted lines correspond to charged and neutral particles, respectively. The directions of the jet axis are indicated as fat bars near the margins of the figures.

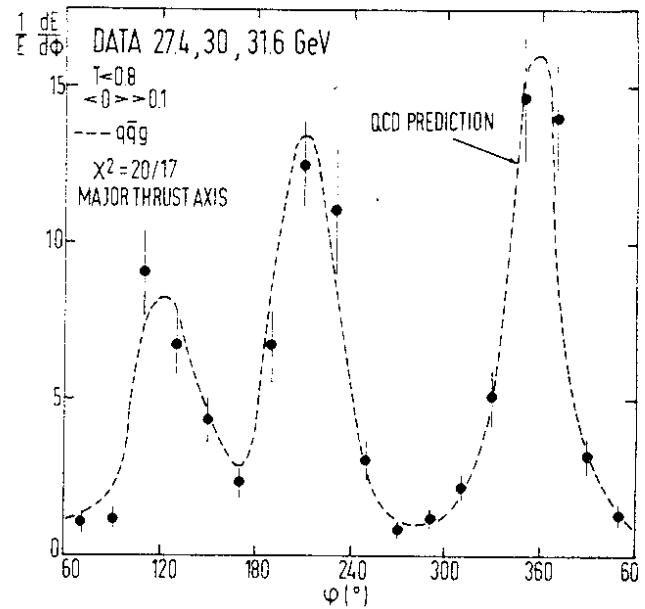
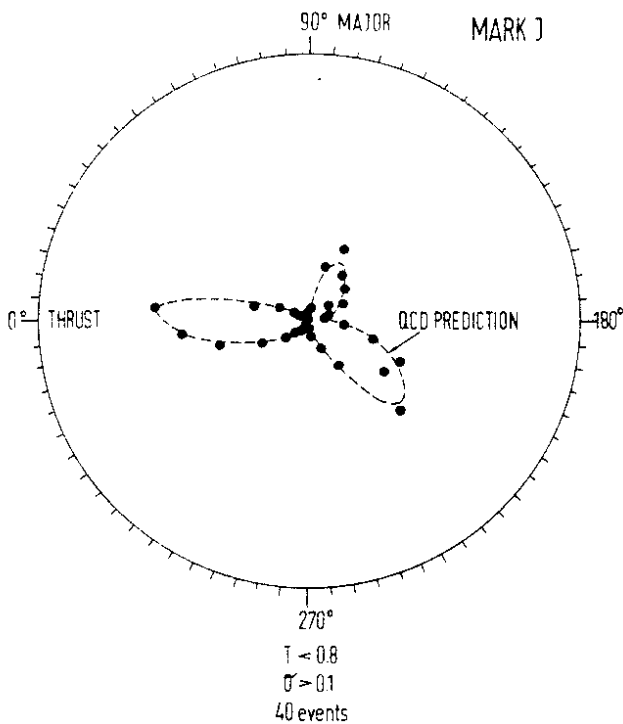
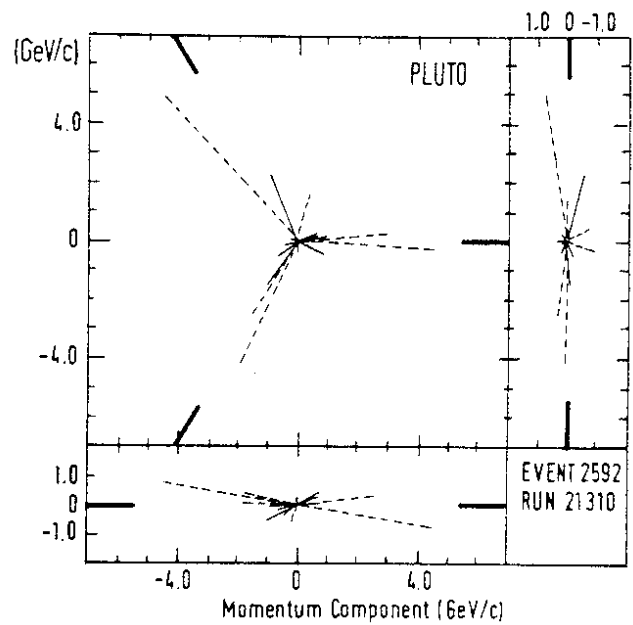


Fig. 23: a) Energy distribution in the event plane. The energy value is proportional to the radial distances. The dashed line is prediction of the $q\bar{q}g$ model.
b) Energy flow in the event plane as function of the polar angle φ .
(MARK J data)

better way the statistical relevance the data are displayed in Fig. 23b as function of the polar angle φ . Statistically the experimental results agree nicely with the gluon emission pattern ($\chi^2 = 67/70$), whereas a simple statistical model is excluded ($\chi^2 = 222/70$). As important is the behaviour of this pattern as a function of thrust T . If events with $T > 0.8$ are selected the small lobe which is supposedly the gluon jet disappears with $T \rightarrow 1$. This is exactly the behaviour predicted by QCD²³⁾.

The final question (point 7) concerns the production rate of gluons. Each experiment has of the order of about 40 flat events. The precise number depends on the particular cuts chosen to select these events. Since these cuts are somewhat different in each experiment it is not possible to take all data together to improve the statistics. For each experiment the number of planar events agrees with the expectation of QCD within the statistical errors.

Finally a consistency check can be made. If the planar events found are due to gluon emission and not to a strange behaviour of the fragmentation process one should expect that the transverse momenta of the hadrons with respect to the 3-jet axis should be normal, i.e. $\langle p_{\perp} \rangle \approx 300$ MeV. In Fig. 24 the distribution^{3,19)} of p_{\perp} relative to the 3-jet axis are shown, and indeed it looks normal.

In conclusion it can be said that evidence for the existence of gluon-bremsstrahlung has been given. One might argue which of the various steps described above was the essential one. Certainly points 5 and 6 are of great relevance. However, it

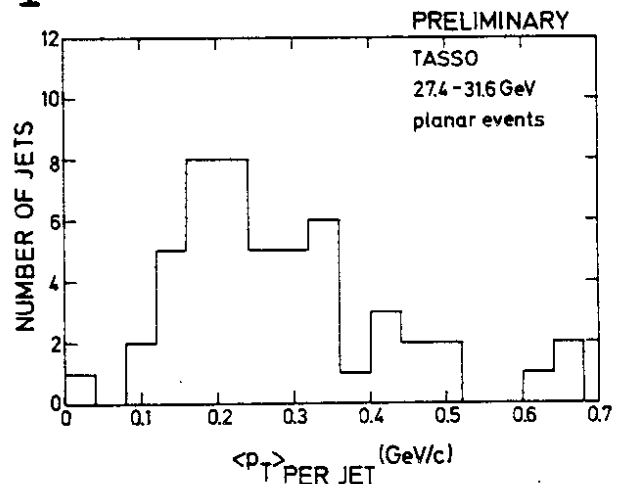


Fig. 24: Distribution of the average p_{\perp} per jet for noncollinear planar events ($S > 0.25$, $3/2 Q_j < 0.04$) analysed as three jet events. (TASSO data.)

is my opinion that it is the sum of all the experimental results mentioned above which make an alternative interpretation very unlikely.

The existence of gluons could be inferred both from the Υ -decay and gluonic bremsstrahlung. From the Υ -decay arguments could also be given for the vector character of the gluon. One essential prediction of QCD remains to be proven, however. This is the self-interaction of gluons due to their colour charge. Unfortunately there exists no easy way to test this phenomenon.

6) Two-photon process

At lower energies e^+e^- annihilation proceeds mainly by one virtual intermediate photon $e^+e^- \rightarrow \gamma \rightarrow \text{hadrons}$. At high energies it is overtaken by an other process where each of the two colliding particles emits a virtual photon and consecutively the photons collide and produce hadrons. One of the interesting aspects of this process is the fact that the hadronic state has charge conjugation $C = +1$ in contrast to one-photon annihilation with $C = -1$. As a consequence different kinds of resonances can be produced.

Experimentally the two processes can be separated quite cleanly either by observing the forward scattered electrons or by cutting on the total visible hadron energy. Whereas in 1-photon processes basically the total c.m. energy goes into hadrons, only a small fraction is available in 2-photon processes since most of the energy is kept for forward going electrons. At PETRA the 2-photon process was first observed by PLUTO²⁴⁾. The photon-photon total cross section is shown as a function of the visible energy in Fig. 25 for a $\langle q^2 \rangle$ value of 0.1 GeV^2 . At high c.m. energies the data agree with the expectation from vector dominance with Regge exchange and including a ρ form factor to account for the virtuality of the photon. Towards lower energies the

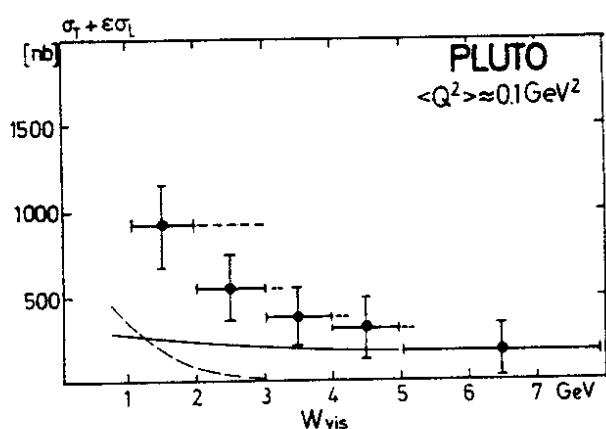


Fig. 25:

The total cross section for 2-photon interactions versus the visible hadron energy W_{vis} at $\langle Q^2 \rangle \approx 0.1 \text{ GeV}^2$. The dashed part of the error bars indicates the range in W that contributes to the data point. The data points are compared to a Regge-exchange model (solid line) and to contributions from pointlike photon-quark couplings (dashed line).

cross section shows a stronger rise than the Regge-model would predict. The difference might at least partly be due to point-like quark-photon couplings even for almost real photons.

Two-photon reactions of the type $e^+e^- \rightarrow \mu^+\mu^-$ have been observed by MARK J¹⁾. The 2-photon processes are a new wide field which has just been opened and which will be an interesting subject to study in the coming years.

7) Search for free quarks

If a new energy regime becomes available by the commissioning of a new accelerator one has to look for free quarks to find out if there is an energy threshold for quark confinement. The JADE experiment cannot only measure the track of a charged particle at 48 different points but can at the same time sample dE/dx at all these points. Knowing dE/dx and p a search for fractionally charged particles has been carried out. No signal has been seen and the preliminary limits^{2,25)} for masses $> 3 \text{ GeV}$ relative to the point-like cross section are $R < 0.08$ for quarks with integer charge and $R < 0.1$ for quarks with $2/3$ charge.

References

1. D.P. Barber et al. (MARK J collaboration), MIT-Report No. 105, August 1979
2. S. Orito (JADE collaboration), Invited talk at 1979 Intern. Symposium at FNAL, and private communication, and DESY-Rep. 79/64 (1979)
3. G. Wolf (TASSO collaboration), DESY-Rep. 79/61 (Sept. 1979) and invited talk at 1979 Intern. Symposium at FNAL
4. E.H. de Groot, D. Schildknecht and G.J. Gounaris, Univ. Bielefeld TP 79/37, November 1979
5. D.P. Barber et al. (MARK J collaboration), MIT-Report No. 104, July 1979
6. D.P. Barber et al. (MARK J collaboration), MIT-Report No. 107, August 1979
7. W. Bartel et al. (JADE collaboration), DESY-Rep. 79/70, October 1979
8. K. Banerjee, contribution to this Symposium
9. B. Anderson et al., Nucl. Phys. B135 (1978), 273
R.D. Field and R.P. Feynman, Nucl. Phys. B136 (1978), 1
10. S. Brandt and H. D. Dahmen, Z. Phys. C1 (1979), 61
11. H. Meyer (PLUTO collaboration), DESY-Rep. 79/81 (1979) and invited talk at 1979 Intern. Symposium at FNAL
12. TASSO-collaboration, DESY-Rep. 79/75, November 1979; similar results have been obtained by other groups
13. D.P. Barber et al. (MARK J collaboration), Phys. Rev. Lett. 43(1979), 901
14. G. Preparata, Phys. Lett. 82B (1979), 398
H. Georgi and D.V. Nanopoulos, Phys. Lett. 82B (1979), 392
H. Harari et al., Phys. Lett. 78B (1978), 459
J.D. Bjorken, SLAC-PUB 2195 (1978)
T.F. Walsh, DESY-Rep. 78/58 (1978)
Y. Muraki et al., Univ. Tokyo, CRL-Rep. 63-78-7 (1978)
N. Krölikovski, Univ. Warszawa (April 1979)
S. Glashow, lecture at DESY, September 1979
15. Ch. Berger et al., Phys. Letters 76B (1978), 243
16. C.W. Darden et al., Phys. Letters 76B (1978), 246 and 78B (1978), 364

17. J.K. Bienlein et al., Phys. Letters 78B (1978),360
18. H. Krasemann and K. Koller, DESY-Rep. 79/52 (1979)
19. R. Brandelik et al.,(TASSO collaboration)
Phys. Lett. 86B (1979),243 and DESY-Rep. 79/53, August 1979
20. Chr. Berger et al.,(PLUTO collaboration)
DESY-Rep. 79/57 (1979) and Phys. Letters 86B (1979),418
21. D.P. Barber et al. (MARK J collaboration)
Phys. Rev. Lett. 43 (1979),830
22. W. Bartel et al. (JADE collaboration),
DESY-Rep. 79/70, October 1979
23. J. Ellis et al., Nucl. Phys. B111,253 (1976),
G. Kramer et al., Phys. Lett. 79B (1978),249
A. de Rujula et al., Nucl. Phys. B138,387 (1978)
24. Chr. Berger et al. (PLUTO collaboration),
DESY-Rep. 79/65, October 1979
25. JADE collaboration, private communication
26. Chr. Berger et al. (PLUTO collaboration),
Phys. Lett. 81B (1979),410
27. Chr. Berger et al. (PLUTO collaboration),
Phys. Lett. 78B (1978),176
28. A. de Rujula et al., Nucl. Phys. B138 (1978),382
29. P. Hoyer et al., DESY-Rep. 79/21 (1979)
30. Chr. Berger et al. (PLUTO collaboration)
DESY-Rep. 79/56 (1979) and Phys. Lett. 86B (1979),413

